

## ANALYSIS OF THERMAL DESORPTION SPECTRA. APPLICATION TO Pd/O<sub>2</sub> SYSTEM

PETAR PERVAN and MILORAD MILUN

*Institute of Physics of the University, 410001 Zagreb, Yugoslavia*

Received 20 February 1986

UDC 538.971

Original scientific paper

Methods for thermal desorption spectra analysis, developed within the Polanyi-Wigner model of thermal desorption kinetics, are reviewed. It is shown that Redhead's method produce substantial errors in calculated energy of desorption. Arrhenius plot method and Chan, Aris and Weinberg's (CAW) method give the energy of desorption  $E$  without the preexponential factor ( $\nu$ ) included in the calculations. These two methods are based on the assumption that  $E$  and  $\nu$  are constants. Using the CAW method as an example we show that these methods can be applied in some circumstances to the systems in which  $E$  depends on coverage. This approach has been tested by the analysis of simulated and experimental (O<sub>2</sub>/polycrystalline Pd) thermal desorption spectra. The experimental spectra are characteristic of the second order kinetics with coverage dependent  $E$ . This dependence may be interpreted as due to the existence of the repulsive lateral interactions in the adsorbed oxygen layer.

### *1. Introduction*

A large number of chemical reactions involve metallic catalysts. Although the empirical set of data on metallic catalysis is significant, there is still a lack of understanding of the processes that take place during the catalytic step of a particular reaction. In order to approach this problem one should take into account the surface conditions of metallic particles, electrodes, etc. involved in the chemical reaction. Firstly, one is interested in the chemical composition of the bare surface

and its structural appearance (defects, grains, patches of segregates etc.), and secondly in how these factors affect the very nature of the surface adsorbate interaction. For example: segregated species may occupy the most favourable adsorption sites on the surface and thus inhibit its catalytic activity; defects could promote some adsorption channels and thus influence the reaction products etc. Therefore, catalytic activity on a metallic surfaces is influenced by a great number of factors and currently can be studied only by considering it as a series of »well-defined« elementary steps under properly defined conditions like ultrahigh vacuum, atomically clean well-defined surfaces, small amounts of reactants of high purity etc. These conditions, since being far from the real situation, cannot give us a complete information on the kinetics and thermodynamics of a particular chemical reaction. However, they enable us to study the elementary steps which constitute these reactions. Such important steps which take place on the surface are: adsorption, dissociation, recombination and desorption etc., and very many spectroscopic techniques have been developed to study each of these processes. Thermal desorption spectroscopy (TDS) is a method enabling one to get some information about the parameters which define the reaction rates of processes occurring on a surface of a catalyst. This method, which has been known since early fifties and modernized in the meantime, is one of the most frequent spectroscopies encountered in the studies of kinetics of desorption of gases adsorbed on various metallic surfaces.

## 2. Theoretical description of desorption rates

Thermal desorption spectroscopy is performed as mass-spectroscopy of reaction products which desorb from a surface whose temperature is increased in the course of time. This method requires ultrahigh vacuum conditions (UHV:  $P < 10^{-7}$  Pa) and this is far from the regime in which the ordinary catalytic reactions take place. Nevertheless, we can extract from thermal desorption spectra information on parameters which determine the rates of reactions in real conditions<sup>1)</sup>. There are altogether four parameters which can be extracted from the TD spectra;

*Order of desorption* ( $m$ ) tells us how the desorption rate depends on the concentration of reactants adsorbed on the surface. This dependence need not necessarily be described by an integer because when the adsorbed particles interact via lateral forces this could, in principle, give rise to any value of  $m$ .

*Activation energy of desorption* ( $E$ ) gives information about the strength of the adsorbate-substrate bond. If the activation energy is of the order of few tenths of eV per bond, then one speaks of physically adsorbed or physisorbed particle. On the other hand, if the activation energy is of the order of 1 eV or more, then the particle is considered to be chemically adsorbed, or chemisorbed on the surface.

*Preexponential factor* ( $\nu^{(m)}$ ) is connected with the vibrational frequency of the adsorbed molecule in the case of first order desorption, and the number of collisions per unit time per unit concentration of adatoms in the case of second order desorption.

*Number of adsorbed particles* ( $N$ ). This may vary between 0 and  $N_0$  where  $N_0$  is the number of active adsorbant sites.

## 2.1. Kinetic equation

In the Polanyi-Wigner model the molecular desorption rate is expressed as<sup>2)</sup>

$$-\frac{dN}{dt} = \nu_0^{(m)} N^m \exp(-E/RT) \quad (1)$$

where  $T$  is substrate temperature and  $R$  is the gas constant. This equation describes the desorption rate in the equilibrium situation in which the surface and the gas are in thermal equilibrium. Although the TDS experiments are usually performed in nonequilibrium conditions (the chemical potential of adsorbed phase  $\mu_a$  is not equal to the chemical potential of gas phase  $\mu_g$ , and the respective temperatures are different) some experiments<sup>3)</sup> have shown that Eq. (1) could also be applied to the nonequilibrium case. If the differential Eq. (1) is divided by  $N_0$  one can write:

$$-\frac{d\Theta}{dt} = \nu_0^{(m)} \Theta^m \exp(-E/RT) \quad (2)$$

where  $\Theta = N/N_0$  is coverage and  $\nu_0^{(m)} = \nu_0^{(m)} N_0^{m-1}$ .

In a real situation, one measures the change of the pressure ( $P$ ) during the desorption experiment. The differential Eq. (3) relates the change of pressure and the pumping speed ( $S$ ) to the desorption rate:

$$\frac{dP}{dt} = -(AkT_g/V) \frac{dN}{dt} - \frac{S}{V} P \quad (3)$$

or

$$\frac{dP}{dt} = -\alpha \frac{d\Theta}{dt} - \frac{P}{\tau} \quad (3a)$$

where  $T_g$  is temperature of the gas phase,  $A$  is substrate area,  $V$  is volume of the system,  $\alpha = AkT_g N_0/V$  and  $k$  is Boltzmann's constant. Instead of the pumping speed we have used in Eq. (3a) the parameter  $\tau$  ( $\tau = V/S$ ) which is the characteristic pumping time, because it can be measured directly by monitoring the rise of pressure when the pump is switched off. When the characteristic pumping time is very short ( $\tau \rightarrow 0$ ), Eq. (3a) reduces to:

$$-P = \alpha \tau \frac{d\Theta}{dt} \quad (4)$$

which provides us with a very useful relationship: the measured pressure is proportional to the desorption rate. Due to this the TDS experiments, whenever possible, are performed in a regime of very short characteristic pumping times. It should be pointed out that the equation (3) does not take into the account readsorption of the desorbing molecules, a process which could be significant only when the characteristic pumping time is very long.

## 2.2. Order of desorption

In the following we shall focus our attention on first and second order desorption kinetics.

### First order kinetics

In the case of first order kinetics, desorption takes place when an adsorbed particle acquires sufficient energy to make an escape from the surface potential well. If linear heating rate is assumed ( $T = T_0 + \beta t$ ), where  $T_0$  is initial temperature and  $\beta$  heating rate, the kinetic equation takes on the form:

$$-\frac{d\theta}{dT} = \frac{\nu_0^{(1)}\theta}{\beta} \exp(-E/RT). \quad (5)$$

The value of the desorption energy usually ranges between ten and few hundred kJ/mol. For the first order desorption kinetics it has been frequently assumed that the preexponential factor is of the order of  $10^{13} \text{ s}^{-1}$ . This assumptions may not hold in all circumstances because some recent experiments have shown<sup>4)</sup> that

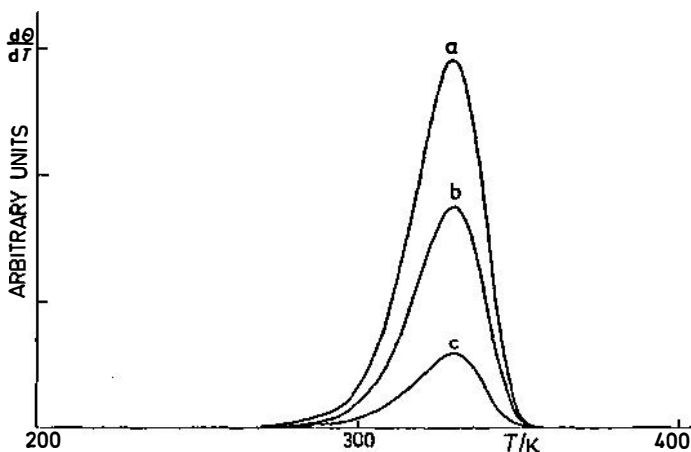


Fig. 1. Calculated desorption rate curves for the first order desorption kinetics.  $E = 83.6 \text{ kJ/mol}$ ,  $\nu = 10^{13} \text{ s}^{-1}$ ,  $\beta = 5 \text{ K/s}$  a)  $\theta_0 = 1$  b)  $\theta_0 = 0.6$  c)  $\theta_0 = 0.2$ .

$\nu$  can vary from  $10^4$  to  $10^{16} \text{ s}^{-1}$ . Fig. 1 shows that for the first order desorption, the temperature  $T_p$ , at which the maximum rate of the desorption occurs, is invariant with respect to the initial coverage  $\theta_0$ . It is seen that the desorption rate curve, in this case, is asymmetric. Hence, the shape of this curve can be, in some situations, used to determine the order of kinetics.

*Second order kinetics*

This type of kinetics is often encountered in the processes in which two adparticles form a desorbing molecule. If the temperature is high enough, two particle collisions give rise to molecular desorption at the rate:

$$-\frac{d\theta}{dT} = \frac{\nu_0^{(2)}\theta^2}{\beta} N_0 \exp(-E/RT) \quad (6)$$

where the preexponential factor  $\nu_0^{(2)}$  is connected with the number of collisions per second per unit concentration of adatoms. Its typical values<sup>5)</sup> range between  $10^{-3}$  and  $10^{-1} \text{ cm}^2 \text{ s}^{-1}$ . In desorption of the second order  $T_p$  depends on the initial coverage. Position of the maximum of the desorption curves shifts to lower values as initial coverage increases (Fig. 2) and the curve is symmetric around  $T_p$  for small  $|T - T_p|$ .

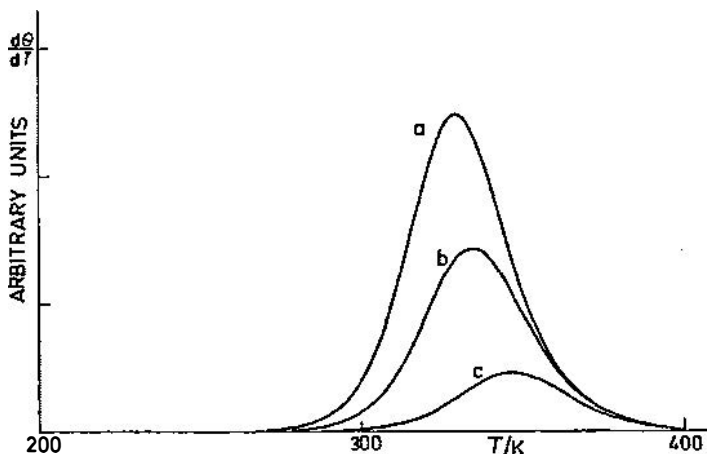


Fig. 2. Calculated desorption rate curves for the second order desorption kinetics:  $E = 83.6 \text{ kJ/mol}$ ,  $\nu = 10^{13} \text{ s}^{-1}$ ,  $\beta = 5 \text{ K/s}$ , a)  $\theta_0 = 1$  b)  $\theta_0 = 0.6$  c)  $\theta_0 = 0.2$ .

Such desorption curve characterizations are correct provided the preexponential factor and the activation energy of desorption are constant. Coverage dependence of  $\nu$  and/or  $E$  changes the lineshapes and the behaviour of desorption curves. Lateral interaction among adsorbed particles can strongly influence the order of desorption<sup>6)</sup>; e. g. the system  $\text{H}_2/\text{Ni} (110)$  exhibits zero order desorption<sup>7)</sup> because of the lateral interaction between adsorbed hydrogen atoms.

*2.3. Activation energy of desorption*

Activation energy of desorption is defined as work required to remove a particle from the surface. Some theoretical works which studied the problem of desorption rates microscopically, showed that the activation energy of desorption need not always be equivalent to the potential well depth<sup>8)</sup>. Energy of desorption for physisorbed molecules (molecules attached to the surface by van der Waals forces) is

40 kJ/mol or less<sup>9)</sup>. For chemisorbed molecules desorption energies range from 50 to 400 kJ/mol<sup>10)</sup>. Fig. 3 shows the influence of the change of energy of desorption on desorption spectra. Even weak lateral interactions between adsorbed particles make the activation energy coverage dependent. In Bragg-Williams model<sup>11)</sup> in which it is assumed that the interaction takes place between pairs of nearest neighbours only, the activation energy of desorption depends linearly on coverage ( $E(\Theta) = E_0(1 + b\Theta)$ ). The parameter  $b$  defines the intensity and the character

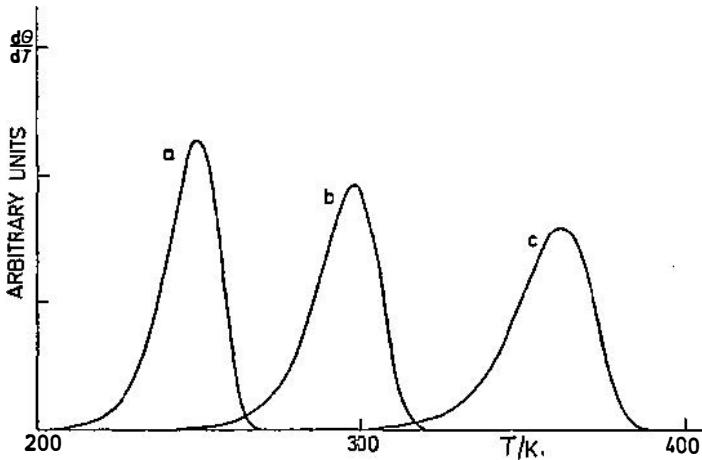


Fig. 3. Calculated desorption rate curves for first order desorption kinetics for different values of activation energy of desorption,  $\nu = 10^{13} \text{ s}^{-1}$ ,  $\beta = 5 \text{ K/s}$ ,  $\Theta_0 = 0.6$  a)  $E = 62.7 \text{ kJ/mol}$  b)  $E = 75.3 \text{ kJ/mol}$  c)  $E = 92 \text{ kJ/mol}$

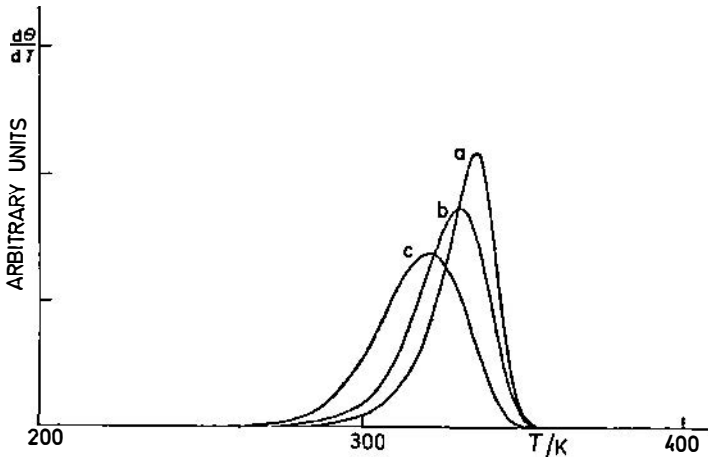


Fig. 4. Calculated desorption rate curves for the first order desorption kinetics with coverage dependent desorption energy:  $E = E_0(1 + b\Theta)$ ,  $E_0 = 83.6 \text{ kJ/mol}$ ,  $\nu = 10^{13} \text{ s}^{-1}$ ,  $\beta = 5 \text{ K/s}$ ,  $\Theta_0 = 0.6$ . (a)  $b = 0.05$  (b)  $b = 0$  (c)  $b = -0.05$ .

of lateral interaction. If  $b$  is greater than zero the interaction is attractive. Fig. 4 shows that for repulsive interactions desorption starts at a lower temperature and the desorption rate curve has a broader peak. On the other hand the attractive interaction results in desorption which starts at higher temperature and the desorption rate curve exhibits very sharp maximum. First order desorption kinetics with small repulsive interaction has initial coverage dependence as second order desorption kinetics with constant activation energy of desorption.

#### 2.4. Preexponential factor

In the simple Frenkel theory of desorption<sup>12)</sup> the preexponential factor for the first order kinetics is the oscillation frequency of adsorbed particles. This is usually assumed to be of the order of  $10^{13} \text{ s}^{-1}$ . As was mentioned before, the experiments have shown that  $\nu$  ranges between  $10^4$  and  $10^{16} \text{ s}^{-1}$ . The explanation for values greater than  $10^{13} \text{ s}^{-1}$  can be given within the transition state theory<sup>13)</sup> in which the preexponential factor can be modified because of the entropy difference between the adsorbed and transition state. This means that desorption of ordered adlayers will be connected with higher values of the preexponential factors. Values lower than  $10^{13} \text{ s}^{-1}$  can be explained by the »weak coupling model«<sup>14)</sup>.

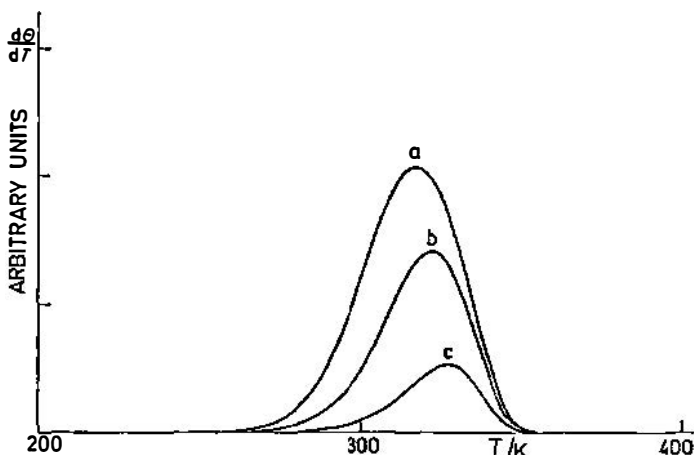


Fig. 5. Calculated desorption rate curves for first order desorption kinetics with repulsive lateral interaction:  $E = E_0 (1 - 0.05 \Theta)$ ,  $E_0 = 83.6 \text{ kJ/mol}$ ,  $\nu = 10^{13} \text{ s}^{-1}$ ,  $\beta = 5 \text{ K/s}$ . a)  $\Theta_0 = 1$  b)  $\Theta_0 = 0.6$  c)  $\Theta_0 = 0.2$ .

Fig. 6 shows the shift in the position of the peak maxima and variation in the magnitude of the peak widths for different values of  $\nu$ . Even very simple theories give the dependence of  $\nu$  on temperature<sup>2)</sup>, but this is usually neglected. Changes in the lineshape and width of the TDS peaks caused by the temperature dependence of the preexponential factor are very small (Fig. 7). The accuracy of the method is insufficient to allow for the extraction of these particular influences from the experimental spectra<sup>15)</sup>. If the adsorbed particles have enough energy to overcome the activation energy for surface diffusion, they will form a two-dimensional gas<sup>5)</sup>.

The model of two-dimensional van der Waals gas introduces the coverage dependence of the preexponential factor<sup>10)</sup> which strongly influences the desorption curves. This is illustrated in Fig. 8.

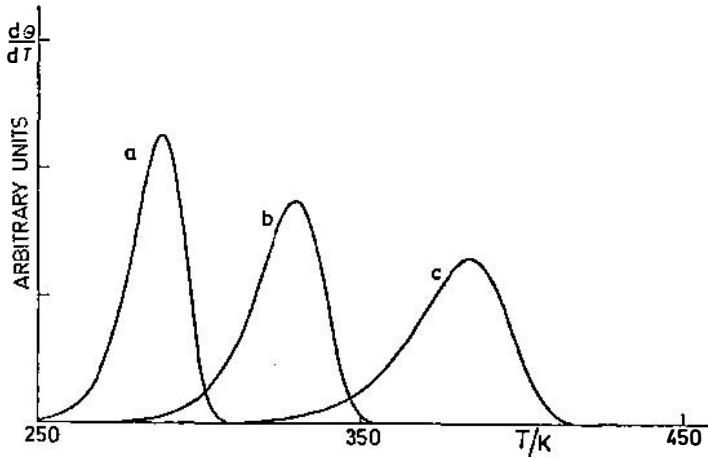


Fig. 6. Calculated desorption rate curves for first order desorption kinetics for different values of the preexponential factor:  $E = 83.6 \text{ kJ/mol}$ ,  $\beta = 5 \text{ K/s}$ ,  $\Theta_0 = 0.6$ . a)  $\nu = 10^{15} \text{ s}^{-1}$ , b)  $\nu = 10^{13} \text{ s}^{-1}$  c)  $\nu = 10^{11} \text{ s}^{-1}$

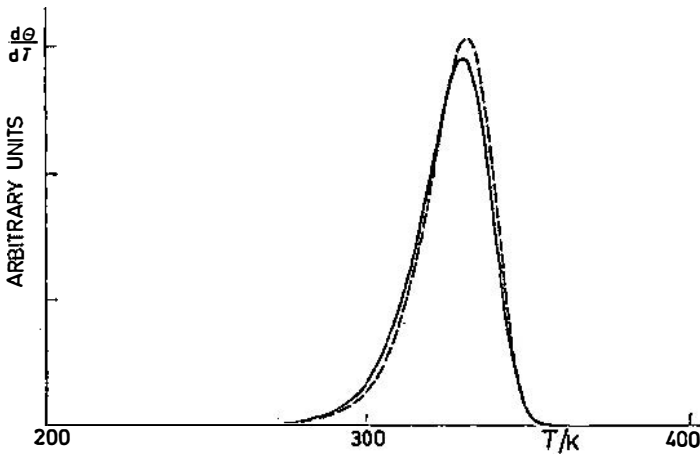


Fig. 7. Calculated desorption rate curves for first order desorption kinetics with  $E_d = 83.6 \text{ kJ/mol}$ ,  $\beta = 5 \text{ K/s}$ ,  $\Theta_0 = 1$ ,  $\nu = 10^{13} \text{ s}^{-1}$  (solid line),  $\nu(T) = (T/T_p)^2 \times 10^{13} \text{ s}^{-1}$  (dashed line),  $T_p = 329 \text{ K}$ .

### 2.5. Effect of heating rate and pumping speed on thermal desorption spectra

The differential equation (3) indicates the importance of the pumping speed for the lineshapes of desorption rate curves. If one makes the substitution  $T = T_0 + \beta t$  in Eq. (3a), then:

$$\frac{dP}{dT} = -\alpha \frac{d\theta}{dT} - \frac{P}{\beta\tau}. \quad (7)$$

Now, it is easy to see that in order to obtain partial pressure as a measure of the desorption rate, the relevant parameter is  $\Omega = 1/\beta\tau$ . Chan et al.<sup>16)</sup> have shown that the approximation  $P \sim d\theta/dT$  is correct only for  $\Omega > 0.5$ . Fig. 9 shows some desorption rate curves for different values of  $\Omega$  (in order to get these pressure

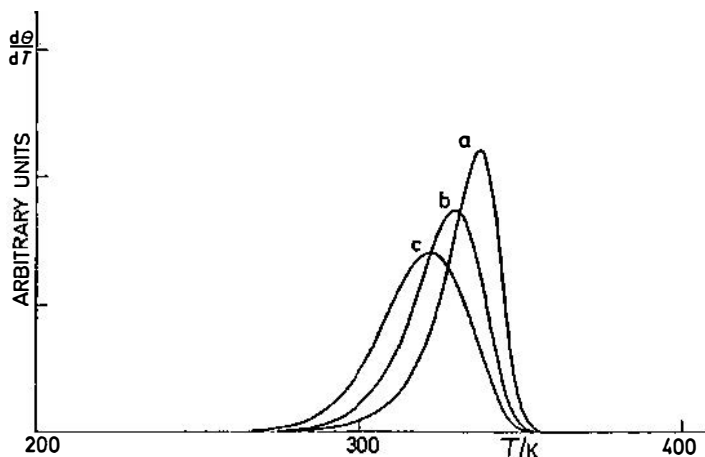


Fig. 8. Calculated desorption rate curves for the first order desorption kinetic with coverage dependent preexponential factor:  $E = 83.6$  kJ/mol,  $\beta = 5$  K/s,  $\theta_0 = 0.6$  and  $\nu = 10^{13} \exp(bE\theta/RT_p)$ ,  $T_p = 329$  K, (a)  $b = 0.05$ , (b)  $b = 0$  and (c)  $b = -0.05$ .

profiles one has to solve the equations (1) and (7) simultaneously). It can be seen that the distortion of the pressure profile is followed by an increase of the peak maximum. Occasionally, one can also ignore the condition  $\Omega > 0.5$  if one wants to increase the signal and use it only as a mere indication that desorption takes place. Sometimes, we are even not able to fulfill this condition because of different pumping speeds for different gases (e. g. the ion pumping speed for inert gases is one hundred times smaller than the pumping speed for nitrogen).

### 3. Analysis of the experimental desorption spectra

In the preceding section we have described the basic parameters which govern the lineshapes, intensity and the position of thermal desorption peaks. A real peak, obtained from a TDS experiment is influenced by all the parameters mentioned

above. It is a task of the analysis to separate these influences and to enable the extraction of the values of the most important parameters: order of kinetics, activation energy of desorption, preexponential factor and their functional dependences on  $\Theta$ . In the following we shall present several methods for desorption trace analysis, as well as some applications on model and experimental spectra.

### 3.1. Methods

(a) The first and probably the simplest analysis has been proposed by Redhead<sup>17</sup>). He started from the assumption that the pumping speed and the heating rate are such that the desorption rate is proportional to the pressure change and that the energy of desorption and the preexponential factor can be considered constant. If one takes the derivative of Eq. (5) and Eq. (6) at  $T_p$ , it follows:

$$\frac{E}{RT_p^2} = \frac{\nu^{(1)}}{\beta} \exp(-E/RT_p), \quad (8)$$

$$\frac{E}{RT_p^2} = \frac{\nu^{(2)} \Theta_0}{\beta} \exp(-E/RT_p), \quad \Theta_0/\Theta_p \approx 2 \quad (9)$$

for the first and second order desorption, respectively. From these relations one can extract the desorption energy by the use of an iterative procedure. In order to do this one has to assume some value for the preexponential factor. The usually assumed value ( $10^{-13} \text{ s}^{-1}$ ) may give rise to a considerable error in the determination of  $E$  (one order of magnitude error in  $\nu$  produces  $\approx 10\%$  error in  $E$ ). The comparison of equations (8) and (9) shows that in the case of second order desorption the temperature of desorption rate maximum depends on initial coverage  $\Theta_0$ . For the first order desorption one can use a simplified relationship for  $T_p$  and  $E$  within the interval  $10^{13} > \nu > 10^8 \text{ s}^{-1}$ , and obtain:

$$\frac{E}{RT_p} = \ln \frac{\nu^{(1)} T_p}{\beta} - 3.64. \quad (10)$$

Assuming the temperature of the peak maximum ( $T_p$ ) and the preexponential factor known this formula can be used to estimate the activation energy of desorption.

(b) The basic advantage of the following method is that the assumption of any value of  $\nu$  is completely avoided. The logarithm of the differential equation (4) gives:

$$\ln \frac{P}{\Theta^m} = \ln(\alpha \tau \nu^{(m)}) - \frac{E}{RT}. \quad (11)$$

If the activation energy and the preexponential factor are constant, the plot of  $\ln(P/\Theta^m)$  versus  $(1/T)$  will give a straight line with the slope  $(-E/R)$ . Interception, equal to  $\ln(\nu^{(m)} \tau \alpha)$ , is used to determine  $\nu$ .

(c) Chan, Aris and Weinberg<sup>18)</sup> developed a simple method to determine the preexponential factor and the activation energy of desorption. In order to carry out calculations,  $T_p$  and the desorption peak width at half maximum  $\Delta W(1/2)$  have to be extracted from the experimental desorption spectra, and no functional dependences of  $E$  and  $\nu$  on  $\Theta$  need be assumed. Hence, for the first order desorption kinetics one has

$$E = RT_p \left[ -1 + \frac{(Y_{1/2}^2 + 5.832)^{1/2}}{Y_{1/2}} \right] \quad (12)$$

$$\nu_0^{(1)} = \beta \frac{E}{RT_p^2} \exp(E/RT_p) \quad (13)$$

where  $Y_{1/2} = \Delta W(1/2)/T_p$ .

Analogously, for the second order desorption kinetics we obtain:

$$E = 2RT_p \left[ -1 + \frac{(Y_{1/2}^2 + 3.117)^{1/2}}{Y_{1/2}} \right] \quad (14)$$

$$\nu_0^{(2)} = \beta \left[ \frac{E}{RT_p} \right]^2 \exp(E/RT_p) \frac{1}{(E/RT_p + 2) \Theta_0 N_0 T_p}. \quad (15)$$

We estimated the accuracy of this method to be within 2% of  $E$ , based on analysis of numerically simulated spectra. Sometimes the methods (a) and (c) are used to analyse the thermal desorption spectra with coverage dependent  $E$ . In this case one starts from a family of thermal desorption curves with different initial coverages. Then, one has to analyze (with the help of equations (8), (9) or (12), (14)) each of these curves, generating thus the desorption energy as a function of initial coverage,  $E(\Theta_0)$  instead of  $E(\Theta)$ . Unfortunately, the function  $E(\Theta_0)$  describes very rarely the real dependence of  $E_d$  on  $\Theta$ .

(d) Habenshaden and Küppers<sup>19)</sup> (HK) have proposed a method which can be termed as »complete« analysis. This method enables one to determine (i)  $E$  without a prior knowledge of  $\nu$ ; (ii)  $\nu$ ; and (iii) their functional dependence on coverage. The first step is the same as in the method explained in (b). If we differentiate equation (4) with respect to  $1/T$  we have:

$$\frac{d(\ln P)}{d(1/T)} = -\frac{E}{R} + \frac{d \ln(\nu^{(m)}/\beta)}{d(1/T)} + \frac{d \ln \Theta^m}{d(1/T)}. \quad (16)$$

Instead of plotting the function  $\ln P$  versus  $1/T$  within a wide range of temperatures HK<sup>19)</sup> have chosen a narrow temperature interval in which the variations of  $\nu$  and  $\Theta$  with  $T$  may be neglected. Within this interval, a plot of  $\ln P$  versus  $1/T$  will give a straight line with the slope  $-E/R$ . Numerical simulations has shown<sup>19)</sup> that the approximation is correct down to the coverage decrease of about

4% from the initial one. If one produces a family of thermal desorption curves, each for different initial coverage, one can analyse them as has been explained previously and determine  $E$  for every curve i. e. for every initial coverage  $\theta_0$ . In this way one gets pairs of  $(E, \theta_0)$  points which will finally form a curve  $E(\theta_0)$ . In contrast to  $E(\theta_0)$  obtained from method (a) and (c),  $E(\theta_0)$  obtained from this method is very close to the function  $E(\theta)$ . In order to determine the preexponential factor, Eq. (5) has to be differentiated with respect to  $\theta$  at  $T = T_p$ :

$$\beta \frac{E}{RT_p^2} \exp(E/RT_p) = \nu m \theta^{m-1} + \theta^m \frac{d\nu}{d\theta} - \nu \frac{\theta^m}{RT_p} \frac{dE}{d\theta}. \quad (17)$$

This differential equation must be solved numerically. If  $\nu$  and  $E$  are constants or if one works in the limit of low coverage, the last two terms on the right hand side of eq. (17) can be neglected after which it reduces to Eq. (8) or (9).

The limitation of this method is that the measurements of pressure and temperature have to be performed in a very short time interval (if the heating rate  $\beta$  is 10 K/s the whole measurement lasts few seconds only). Numerical simulations<sup>19)</sup> have shown that this time, i. e. temperature interval, decreases as the desorption energy decreases. Nowadays, this problem is not a too serious one any more as the computer processing of the data is readily available.

### 3.2. Applications

In this section we shall demonstrate the application of the methods for analysis of thermal desorption studied in Section 3.1. to some specific systems. In the first two examples we shall generate numerically the thermal desorption spectra of the first order. Comparing the evaluated and assumed values of the desorption energy and the preexponential factor one can estimate the accuracy of the methods in the most favorable situation when the experimental errors and surface imperfections are absent. The third example is the analysis of real thermal desorption spectra, which we recorded in desorption of  $O_2$  from polycrystalline palladium.

#### *Example 1. Constant $E$ . Numerically generated spectra.*

We generated numerically a test desorption curve of the first order using Eq (5) and putting  $E = 83.6$  kJ/mol,  $\nu = 10^{14} \text{ s}^{-1}$  and  $\beta = 5$  K/s. This gives  $T_p = 305$  K. Using Eq. (8) and assuming the preexponential factor  $\nu = 10^{13} \text{ s}^{-1}$ , the method (a) gives  $E = 77.6$  kJ/mol. The 7% error in calculated  $E$  is due solely to the erroneously chosen value of the preexponential factor. Using the method (b) we analysed the desorption curve in the temperature interval 278–322 K. The plot of  $\ln(P/\theta)$  versus  $1/T$  gives  $E = 84$  kJ/mol and  $\nu = 1.16 \times 10^{14} \text{ s}^{-1}$ . For the method (c) one has to know  $T_p$  and  $\Delta W(1/2)$  and we found that  $\Delta W(1/2) = 21.5$  K. Substituting these values into Eqs. (12) and (13) we found  $E = 83.8$  kJ/mol and  $\nu = 1.24 \times 10^{14} \text{ s}^{-1}$ . In the method (d) we chose the temperature interval between 250 and 298 K within which the coverage decreases from the initial value by 4%. Using Eqs. (16) and (17) we evaluated  $E = 83$  kJ/mol and  $\nu = 9.8 \times 10^{13} \text{ s}^{-1}$ .

#### *Example 2. Coverage dependent $E$ . Numerically generated spectra.*

In this example we consider the coverage dependent energy of desorption:  $E(\theta) = E_0(1 + b\theta)$ . It will be shown that in this situation the methods (a), (b) and (c)

are inapplicable or, if one uses them, it must be done with a great care. We assume  $E_0 = 83.6$  kJ/mol,  $\nu = 10^{12} \text{ s}^{-1}$ ,  $b = 0.05$  and  $\beta = 5$  K/s. Using Eq. (5) we numerically generated the thermal desorption spectra for various initial coverages. The results of the analyses are given in Table 1. Here, the plot  $\ln(P/\theta)$  versus  $1/T$  (method (b)) did not produce straight line. For this reason we haven't included the method (b) in Table 1. It can be seen that the results obtained by method (c) strongly deviate from the test desorption energies for higher coverages, but for smaller coverages it gives better results than method (a). Attractive lateral interactions, which are included in this model, cause the narrowing of the desorption curves, and shift  $T_p$  towards higher temperatures. Due to this, the parameter  $Y_{1/2} = \Delta W(1/2)/T_p$  is strongly affected, and so is the energy of desorption given by Eq. (12). The method (a) uses  $T_p$  as a free parameter for the evaluation of  $E$ , and even with incorrectly assumed preexponential factor gives substantially better results for higher coverages. The method (d) is, as we have expected, more accurate in this situation. We analyzed the points from »4% coverage decrease« temperature interval (from 327 to 374 K). The choice of the narrower temperature interval could give a better agreement but in the case of real spectra the analysis must account for the effects of statistics. The plot of  $E(\theta_0)$  versus  $\theta_0$  gives  $E_0 = 82.4$  kJ/mol and  $b = 0.07$ .

TABLE 1.

	method (a)	method (c)	method (d)	$E_0(1 + b\theta_0)$
$E(\theta_0 = 1)$ kJ/mol	93	141	88.2	87.8
$E(\theta_0 = 0.75)$	92.2	122.6	86.8	86.7
$E(\theta_0 = 0.50)$	91.4	108	85.4	85.7
$E(\theta_0 = 0.30)$	90.6	97.7	84	84.8
$E(\theta_0 = 0.10)$	89.9	87	83.2	84

Numerically generated spectra ( $E = 83.6(1 + 0.05\theta_0)$  kJ/mol;  $\nu = 10^{12} \text{ s}^{-1}$ ;  $\beta = 5 \text{ K s}^{-1}$ ) have been analysed using methods (a), (c) and (d). The results of analysis are given for different initial coverages together with the corresponding test energies  $E_0(1 + 0.05\theta_0)$ .

### Example 3. Analysis of the experimental spectra $\text{O}_2/\text{Pd}$ (polycrystal)<sup>20)</sup>

The situation is more complicated if the analysis of a real spectrum is made. Our experimental spectra describe the desorption of molecular oxygen from polycrystalline palladium. In this situation one can expect a more complex spectrum because the desorption is influenced by the presence of different crystallographic orientations on the surface of the sample (and therefore different desorption energies), surface defects, roughness etc. Fig. 10 shows a family of desorption curves obtained experimentally for different initial coverages<sup>20)</sup>. As is well known that oxygen adsorbs dissociatively on monocrystal Pd surfaces at temperatures above  $150 \text{ K}^{22)$ , one may expect second order desorption in the present case as well. This is in agreement with the behaviour of our desorption curves.

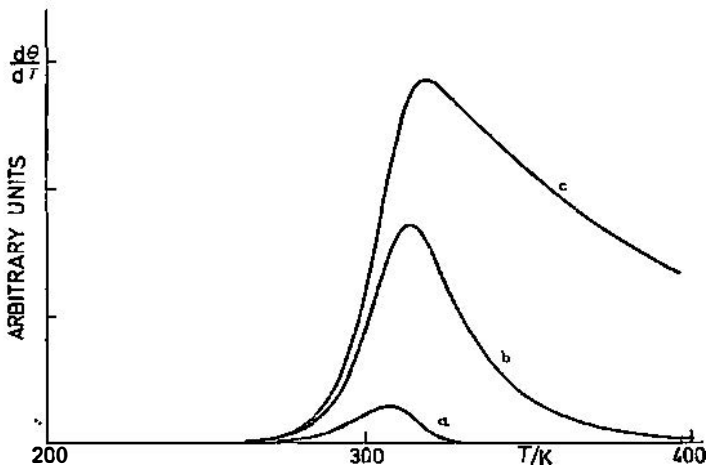


Fig. 9. Calculated pressure profiles for different values of  $\Omega$  and  $E = 83.6 \text{ kJ/mol}$ ,  $\nu = 10^{13} \text{ s}^{-1}$ ,  $\theta_0 = 1$ . (a)  $\Omega = 0.5$ , (b)  $\Omega = 0.05$  and (c)  $\Omega = 0.01$ .

The plot of  $\ln(P/\theta^2)$  versus  $1/T$  is not a straight line which indicates that the spectrum is not a simple one and is probably a sum of several desorption spectra. Also, the lateral interactions probably play some role at higher coverages. The width of the peak is strongly affected by these effects and one can expect some problems in trying to analyse the spectra by method (c). As can be seen in the Table 2, the energy of desorption obtained by method (c) changes drastically with initial coverage. In contrast to Example 2, here the energy of desorption increases with the decrease of initial coverage, and this indicates possible occurrence of repulsive lateral interactions. Because of the lack of computer data processing we were not able to apply the method (d) and investigate this assertion. However, as the initial coverage decreases the probability that only one kind of sites will accommodate oxygen atoms increases (which implies a single desorption energy) and in the limit of small  $\theta_0$  the lateral interactions can be neglected. The analysis of the desorption spectrum

TABLE 2.

initial coverage	method (a)		method (c)	
	$E \text{ (kJ/mol)}$	$\nu \text{ (s}^{-1}\text{)}$	$E \text{ (kJ/mol)}$	$\nu \text{ (s}^{-1}\text{)}$
0.9	211.3	$10^{13}$	171.5	$2.3 \times 10^{10}$
0.57	210.7	„	193.5	$7.2 \times 10^{10}$
0.48	210.8	„	206.2	$4.8 \times 10^{12}$
0.2	210.7	„	218.3	$2.8 \times 10^{13}$
0.11	210.2	„	226.0	$8.6 \times 10^{13}$

Desorption energy  $E$  and preexponential factor  $\nu$  calculated by the use of the method (a) with assumed value of  $\nu$  and method (c) for spectra shown in Fig. 10.

with  $\Theta_0 = 0.11$  by method (c) gives  $E = 226$  kJ/mol and  $\nu = 8.6 \times 10^{13} \text{ s}^{-1}$ , which is in excellent agreement with  $E = 230$  kJ/mol for desorption of oxygen from Pd (111)<sup>2,1)</sup> and  $E = 228$  kJ/mol for desorption of oxygen from Pd (331) at low coverages<sup>2,3)</sup>. For the same initial coverage ( $\Theta_0 = 0.11$ ) the method (a) gives lower energy of desorption  $E = 210$  kJ/mol but we obtained this by assuming  $\nu = 10^{13} \text{ s}^{-1}$ . If we substitute in Eq. (9) the preexponential factor  $10^{14} \text{ s}^{-1}$  we get  $E = 230$  kJ/mol. Spectra taken in the saturation limit (complete monolayer formation) can be used for the estimation of the energy of lateral interaction<sup>2,4)</sup>.

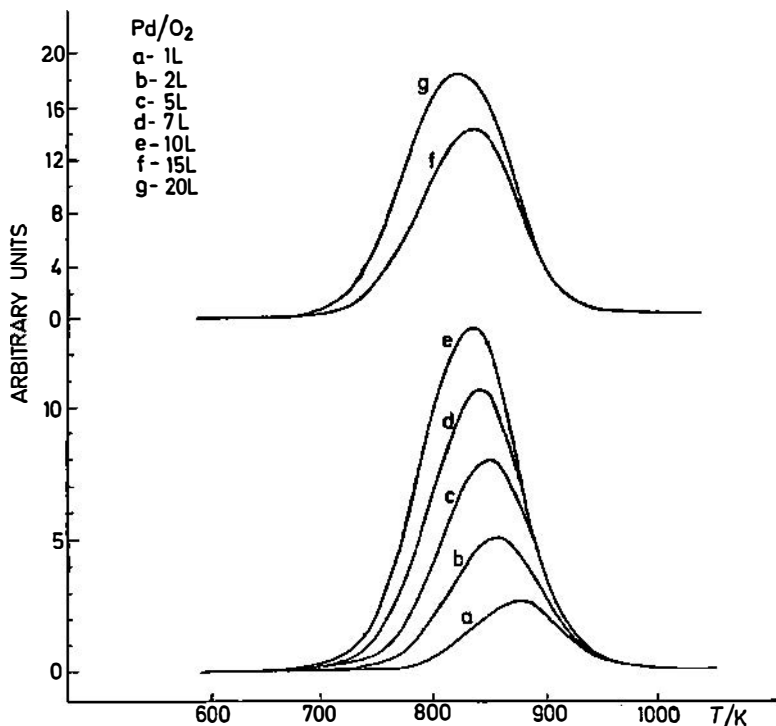


Fig. 10. TD spectra of  $\text{O}_2/\text{Pd}$  (polycrystalline foil) system taken after various exposures at 300 K substrate temperature.

It can be shown that for lateral energies up to 10% of the total desorption energy, linear relationship exists between parameter  $Y$  (method (c)) and parameter  $b$ . Using this relationship we obtained  $b = 0.05$ , which in our case (polycrystalline surface) includes not only lateral interaction contribution to the desorption energy, but also the effect of a large number of adsorption sites possessing slightly different desorption energies.

#### 4. Conclusions

Desorption processes in which  $E$  and  $\nu$  may be considered as constant will yield the TD spectra amenable to the analysis by means of the methods (a), (b) and

(c) described in this paper. Among these, the method (c) seems to exhibit some advantage with respect to the other two, mainly because of its simplicity and accuracy.

In the cases where the coverage dependence of  $E$  and  $\nu$  exists, the method proposed by Habenschaden and Küppers may be recommended. Unfortunately, this method needs a great number of experimental points in a narrow temperature interval. Because of that, and if no computer acquisition of data is available the method is not practical. On the other hand, the method (c) could be applied to the problem but only in the low initial coverage regime. In the combination with  $Y/b$  relationship it is possible to obtain the functional dependence of  $E(\theta)$  if the relationship  $E = E_0(1 + b\theta)$  holds.

Desorption of oxygen adsorbed at room temperature from the polycrystalline palladium foil obeys second order kinetics. The activation energy of desorption is coverage dependent. Strong indication ( $b = -0.05$ ) has been found that the repulsive lateral interaction influences desorption energy.

#### Acknowledgment

We would like to acknowledge the support obtained from the International Atomic Energy Agency (Vienna)-(RC 3227), the Aleksander von Humboldt Stiftung (Bonn)-(V-8141 and V-8151), and the Internationales Büro der KFA Jülich (32.2. A. F.).

#### References

- 1) P. Stoltzer and J. K. Nørskov, *Phys. Rev. Lett.* **55** (1985) 242;
- 2) H. Ibach, E. Ertey and H. Wagner, *Surface Sci.* **92** (1980) 29;
- 3) G. Comsa, in *Proc. 7th Intern. Vacuum Congr. and 3rd Intern. Conf. on Solid Surfaces* Vienna, 1977 p. 1317.;
- 4) C. G. Goymour and D. A. King, *J. Chem. Soc. Faraday Trans.* **168** (1972) 280  
C. Kohrt and R. Gomer, *Surface Sci.* **24** (1971) 77;
- 5) J. T. Yates, *The Chemical Physics of Solid Surfaces and Heterogeneous Catalysis*, Elsevier, 1982;
- 6) A. Cordoba and J. J. Luque, *Phys. Rev. B* **26** (1982) 4028;
- 7) K. Christman, O. Schaber, G. Ertl and M. Neuman, *J. Chem. Phys.* **60** (1974) 4528;
- 8) B. Helsing, *J. Chem. Phys.* **83** (1985) 1371;
- 9) J. T. Yates and N. E. Ericsson, *Surface Sci.* **44** (1974) 489;
- 10) F. C. Tompkins, *Chemisorption of Gases on Metals*, Academic Press, 1978, London;
- 11) W. L. Bragg and E. J. Williams, *Proc. Roy. Soc. A* **145** (1934) 699;
- 12) I. Frenkel, *Z. Phys.* **26** (1924) 117;
- 13) A. Redondo, Y. Zeiri, J. J. Low and W. A. Goddard III, *J. Chem. Phys.* **79** (1983) 12;
- 14) K. C. Janda, J. E. Hurst, C. A. Becker, J. P. Cowin, D. J. Auerbach and L. Wharton, *J. Chem. Phys.* **72** (1980) 2404;
- 15) J. M. Soler and N. Garcia, *Surface Sci* **124** (1983) 563;
- 16) C. M. Chan and W. H. Weinberg, *Appl. Surface Sci.* **1** (1978) 377;
- 17) P. A. Redhead, *Vacuum* **12** (1962) 203;
- 18) C. M. Chan, R. Aris and W. E. Weinberg, *Appl. Surface Sci.* **1** (1978) 360;
- 19) E. Habenschaden and J. Küppers, *Surface Sci. Lett.* **138** (1984) L147;
- 20) M. Milun, P. Pervan and K. Wandelt, to be published;
- 21) H. Conrad, G. Ertl and J. Küppers, *Surface Sci.* **65** (1977) 235;
- 22) T. Matsushima, *Surface Sci.* **157** (1985) 297;
- 23) P. W. Davies and R. M. Lambert, *Surface Sci.* **110** (1981) 227;
- 24) P. Pervan and M. Milun, to be published.

ANALIZA SPEKTARA TERMALNE DESORPCIJE. PRIMJENA NA  
SISTEM Pd/O<sub>2</sub>

PETAR PERVAN i MILORAD MILUN

*Institut za fiziku Sveučilišta, 41000 Zagreb*

UDK 538.971

Originalni znanstveni rad

U prvom dijelu rada dani su osnovni elementi teorije termalne desorpcijske spektroskopije i karakterizacija spektara koji slijede kinetiku prvog i drugog reda. Prikazane su četiri metode analize desorpcionih spektara, razvijene u okviru Polanyi-Wigner modela termalne desorpcije. Pokazano je da Redhead metoda u nekim slučajevima može proizvesti značajnu pogrešku kod određivanja energije desorpcije. »Arrhenius plot« i Chan, Aris & Weinberg metode daju energiju desorpcije bez poznavanja preeksponencijalnog faktora. Iako su te metode razvijene pod pretpostavkom da su  $\bar{E}$  i  $\nu$  konstante pokazano je da se i te metode u određenim slučajevima mogu koristiti kod sistema gdje  $E$  ovisi o pokrivenosti. Metode su testirane analizom numerički generiranih i jednog experimentalno dobivenog spektra (O<sub>2</sub>/polikristalični paladij). Analiza eksperimentalnog spektra ukazuje na kinetiku drugog reda te da energija ovisi o pokrivenosti, vjerojatno zbog postojanja odbojnog međudjelovanja adsorbiranih atoma kisika.